Atmos. Meas. Tech. Discuss., 4, 73–99, 2011
www.atmos-meas-tech-discuss.net/4/73/2011/
doi:10.5194/amtd-4-73-2011

Atmospheric Measurement Techniques Discussions

Inter-comparison of lidar and ceilometer retrievals for aerosol and Planetary Boundary Layer profiling over Athens, Greece

G. Tsaknakis[1], A. Papayannis[1], P. Kokkalis[1], V. Amiridis[2], H. D. Kambezidis[3], R. E. Mamouri[1], G. Georgoussis[4], and G. Avdikos[4]

[1]Laser Remote Sensing Unit, Department of Physics, National Technical University of Athens, Heroon Polytechniou 9, Zografou Campus, 15780 Athens, Greece
[2]Institute for Space Applications and Remote Sensing, National Observatory of Athens, Greece
[3]Atmospheric Research Team, Institute of Environmental Research and Sustainable Development, National Observatory of Athens, Lofos Nymphon, 11810 Athens, Greece
[4]Raymetrics S.A., Papathanasiou 12, 19002 Paiania, Athens, Greece

Received: 23 November 2010 – Accepted: 23 December 2010 – Published: 10 January 2011

Correspondence to: A. Papayannis (apdlidar@central.ntua.gr)

Published by Copernicus Publications on behalf of the European Geosciences Union.

Abstract

This study presents an inter-comparison of two active remote sensors (lidar and ceilometer) in determining the structure of the Planetary Boundary Layer (PBL) and in retrieving tropospheric aerosol vertical profiles over Athens, Greece. This inter-comparison was performed under various strongly different aerosol concentrations (urban air pollution, biomass burning and Saharan dust event), implementing two different lidar systems (one portable Raymetrics S.A. lidar system running at 355 nm and one multi-wavelength Raman lidar system running at 355 nm, 532 nm and 1064 nm) and one CL31 Vaisala S.A. ceilometer (running at 910 nm). To convert the ceilometer data to data having the same wavelengths as those from the lidar, the backscatter-related Ångström exponent was estimated using ultraviolet multi-filter radiometer (UV-MFR) data. The inter-comparison was based on two parameters: the mixing layer structure and height determined by the presence of the suspended aerosols and the aerosol backscatter coefficient. Additionally, radiosonde data were used to derive the PBL height. In general a good agreement is found between the ceilometer and the lidar techniques in both inter-compared parameters in the height range from 500 m to 5000 m, while the limitations of each instrument are also examined.

1 Introduction

The Planetary Boundary Layer (PBL) being the lowest part of the troposphere is directly influenced by the earth's surface, solar irradiance and anthropogenic activities. Thus, air pollution concentrations in the PBL are generally orders of magnitude higher than those in the free troposphere (Stull, 1988). Additionally, heat and moisture from the surface must first be mixed through the PBL before being available to the circulation of the free troposphere. Consequently, studies of atmospheric dynamics in the troposphere very frequently employ PBL height data. Moreover, the influences of anthropogenic activities and earth's surface upon air quality can be monitored by studying

AMTD
4, 73–99, 2011

the aerosol concentration and their relevant optical-microphysical and chemical properties (Seinfeld and Pandis, 2006).

Laser remote sensing techniques (lidars and ceilometers) are proven to be powerful tools for tracking and monitoring the evolution of the PBL height (Papayannis and Balis, 1998; Amiridis et al., 2007), as well as the vertical profiles of aerosol properties over long time periods (Amiridis et al., 2005). The backscatter intensity of the returned signal depends mainly on the particulate concentrations in the air. As the size of particles varies with their moisture content, the reflectivity is influenced also by atmospheric humidity (Angelou et al., 2010). Therefore, the lidar techniques are useful for three dimensional mapping of aerosols, remote sensing of ambient air pollutants, industrial emissions, and natural aerosol emissions due to volcanoes eruptions (Wang et al., 2008), biomass burning (Amiridis et al., 2009) and desert dust transport events (Papayannis et al., 2008, 2009). On the other hand, ceilometers are devices used mostly for measuring the height of cloud bases by aerosol detection (Martucci et al., 2010).

Both lidars and ceilometer involve laser light backscattering measurements to determine the aerosol backscatter coefficient (Klett, 1981) and thus, to obtain the cloud base (Martucci et al., 2010) or the PBL height (Eresmaa et al., 2006; McKendry et al., 2009; Heese et al., 2010). The difference between the two instruments is that the laser light source used in ceilometers is much weaker and broader spectrally compared to that of a lidar system, which limits the ability of ceilometers to detect aerosols up to 3 km, according to Markowicz et al. (2008). Recently, Heese et al. (2010) compared aerosol backscatter coefficient profiles retrieved by a new generation CHM15K-X Jenoptik ceilometer and the IfT's lidar Polly in Leipzig (Germany) and suggested that the ceilometer is able to detect aerosol layers in the PBL and also in the free troposphere up to altitudes of the order of 4 km.

In this study aerosol backscatter coefficient profiles obtained by a CL31 ceilometer (from Vaisala S.A.) owned by the National Observatory of Athens were evaluated against quality assured aerosol profiles obtained by the National Technical University of Athens (NTUA) and Raymetrics S.A. lidar systems, over a highly polluted urban site,

AMTD
4, 73–99, 2011

such as the Athens Basin. The data were obtained under various strongly different aerosol-type presences (urban pollution, biomass burning and Saharan dust event). Section 2 briefly presents the instrumentation involved in this study. Sections 3 and 4 show an inter-comparison of the PBL height and the aerosol backscatter coefficient, respectively, as retrieved by ceilometer and lidar measurements. Finally, Sect. 5 presents our conclusions.

2 Instrumentation

2.1 Ceilometer

The ceilometer used in this study was a Vaisala CL31 model. It is equipped with an InGaAs MOCVD pulsed diode laser. The wavelength of the emitted laser beam is 910 nm and the energy per pulse is 1.2 µJ. The emission frequency is 10 kHz, while the pulse duration is 100 ns. The elastically backscattered radiation is collected by a lens, which plays the role of the receiving optics. The inner part of the lens is used for the alignment of the instrument and for the laser beam emission, while the outer part is used for the collection and focusing of the backscattered radiation onto the receiver. The full overlap height of the instrument is achieved for altitudes higher than 50 m. The separation between the two areas is achieved by an oblique mirror. The backscattered data are acquired and stored by a 60 MHz digital processor and stored in a hard disk unit. The aerosol backscatter coefficient is obtained from 50 m up to 7.5 km height with a spatial resolution of 5 m and a temporal resolution of 2 s (http://www.vaisala.com). The full overlap height of the instrument is achieved for altitudes higher than 10 m.

2.2 Lidar systems

The Raymetrics S.A. lidar system is a portable eye-safe elastic backscatter lidar system, fully automated. It can work 24 h per day outdoors in an unattended mode under

AMTD
4, 73–99, 2011

almost any weather conditions. A pulsed laser beam at 355 nm is emitted into the atmosphere. The energy per emitted pulse is 40 mJ, while the pulse duration is 10 ns. A beam expander is used at the emission unit in order to expand the laser beam by a factor of 10, so that the eye safety is completely fulfilled. The repetition rate is 10 Hz. The backscattered radiation is collected by a Cassegrain telescope of 200 mm in diameter. The collected radiation is spectrally analyzed (using beam splitters), filtered (using narrow band interference filters) and focused on photomultiplier tubes (PMTs) which are used to detect the received lidar signals in the analog and the photon counting mode. The corresponding raw signal spatial resolution is 3.75 m and the temporal resolution was fixed at 5 min. The full overlap height of the instrument is achieved for altitudes higher than 100 m.

The NTUA lidar system is a multi-wavelength Raman lidar based on a compact pulsed Nd:YAG laser, emitting simultaneously at 1064, 532 and 355 nm with output laser-beam energies of 400, 150 and 75 mJ per pulse, respectively. The repetition rate is 10 Hz. The optical receiver is a Cassegrain-reflecting telescope with a primary mirror of 300 mm in diameter and a focal length $f = 600$ mm, directly coupled, through an optical fiber, to the lidar signal detection box (Mamouri et al., 2007). The lidar signals are detected with photomultiplier tubes (PMTs) operating both in the analog and photon-counting mode. The corresponding spatial resolution of the detected raw signals is 7.5 m. The NTUA lidar detects both elastic backscattered (at 1064, 532, 355 nm) and Raman (at 607 and 387 nm-nitrogen and 407 nm-water vapor) signals. The lidar operates in the frame of EARLINET project since 2000, while the algorithms implemented for the data acquisition and processing were successfully inter-compared (Böckmann et al., 2004; Matthias et al., 2004; Pappalardo et al., 2004). The NTUA lidar system can provide continuous measurements of the aerosol backscatter vertical profiles ranging from 1000 m up to 15 000 m height. For this study the time resolution of the retrieved aerosol profiles was fixed at 1.5 min, while the spatial resolution at 15 m. The full overlap height of the instrument is achieved for altitudes higher than 1000 m.

AMTD
4, 73–99, 2011

2.3 Multi filter radiometer

The ultraviolet Multi Filter Radiometer (UV-MFR) measures the total, diffuse and direct solar radiation. The spectral measurements are performed in 6 wavelengths and a wide-band channel. The total and the diffuse radiation are measured directly while the direct radiation is calculated as the difference between the two. The spectral width of the UV-MFR optical filters is 10 nm (FWHM) at 415, 500, 615, 671, 867, 940 nm. The cosine response is 5% for zenith angles between 0° and 80°. The instrument is designed to perform continuous measurements for external temperatures ranging from −30 to +50 °C since the electronics and the photodiodes are enclosed in a thermally controlled box.

3 Inter-comparison of Planetary Boundary Layer height determination using ceilometer and lidar measurements

The CL31 ceilometer and the Raymetrics lidar were combined and collocated for two days (26–27 November 2008) in order to perform measurements over Athens. Both instruments were located nearby the actinometric station of the National Observatory of Athens on the hill of Pnyx (37°58′19.46″ N, 23°43′05.82″ E), 100 m a.s.l. The ceilometer was operated on a 24-h basis, while the lidar for selected time periods within the above two days. All data are presented in Universal Time Coordinated (UTC).

In Fig. 1a we present the temporal evolution of the backscattered signal (in arbitrary units-A.U.) at 910 nm as obtained by the ceilometer on 26 November, between 10:15 and 13:45 UTC, with a 10 min time resolution (based on 2 s raw time resolution signals). In Fig. 1b and c we show the temporal evolution of the range-corrected backscattered lidar signal and the corresponding first derivative of the logarithm of the range-corrected lidar signal at 355 nm (in A.U.), respectively, as obtained by the Raymetrics lidar from 10:15 to 13:45 UTC on the same day. The same procedure was followed during the next day on 27 November, where simultaneous measurements were obtained from 08:40

AMTD
4, 73–99, 2011

to 11:35 UTC (Fig. 2a–c). Along with the ceilometer and lidar data, radiosoundings were performed at a nearby location by the Hellenic National Meteorological Service (HNMS) at 12:00 UTC to determine the PBL height. Thus, Fig. 3a and b presents the vertical profile of the relative humidity (%) and the potential temperature (K) for 26 and 27 November, respectively.

To retrieve the PBL height we used both radiosounding and lidar data, according to the methodologies provided by Stull (1988) and Menut et al. (1999), respectively. In the first case, the strong negative gradient of the relative humidity, along with the positive gradient of the potential temperature delineate the position of the PBL height. In the latter case, the PBL height is found where the minimum of the first derivative of the logarithm of the range-corrected lidar signal occurs. In our case we used the first derivative only for the lidar signals, since for the ceilometer data this quantity was not available to us. When only the aerosol backscatter coefficient data are available (in our case the ceilometer data) we can still derive the PBL height, since its maximum height is very frequently associated with a strong gradient in the vertical aerosol profile (Endlich et al., 1979; Menut et al., 1999).

According to the ceilometer data (Fig. 1a) the PBL height on 26 November ranged between 0.65 to 0.8–0.85 km a.s.l. (light blue color) and remained practically constant around 0.85 km after 12:30 UTC. The internal part of the PBL (Stull, 1988) is represented by the light green color structure, which is located around 500–600 m. The corresponding range-corrected backscattered lidar data (in A.U.) at 355 nm provided by the Raymetrics system (Fig. 2b) showed a similar structure, where the PBL height is depicted as the top of the light blue zone, located around 800–850 m a.s.l. The internal part of the PBL is represented by the light green color structure, which is located around 600–650 m. This becomes more visible in the temporal evolution of the first derivative of the logarithm of the range-corrected lidar signal (Fig. 2c) where the zones of dark blue colors delineate the PBL height (ranging from 800–900 m). As a first conclusion, comparing the three graphs of Fig. 1a–c, we can say that both systems revealed a very similar PBL structure (with a difference of about 50–100 m), when the

AMTD
4, 73–99, 2011

same time period of measurements is considered. However, when we consider the vertical profiles of the relative humidity and the potential temperature for that day from the radiosonde (Fig. 3a), we clearly see the presence of two layers, according to the criteria mentioned previously: the first up to 1450 m and the second around 2000 m height. This is a case where there is an important discrepancy between the retrieved PBL height. This difference may be attributed to the fact that the lidar and the radiosonde measurements were not collocated (they were at a distance of about 6 km), thus not the same air masses were sampled.

Next day's ceilometer's measurements (Fig. 2a) showed that the PBL height ranged from 550 m (around 09:00 UTC) to 1250–1300 m (around 10:20 UTC) (light orange-yellow color structure). The corresponding lidar measurements (Fig. 2b and c) showed that the PBL height ranged from 550 m (around 09:00 UTC) to 1300–1400 m (around 11:30 UTC), which is a typical evolution of the PBL due to increased solar irradiance (Stull, 1998). This evolution is more clearly visible in Fig. 2c by the deep blue color scale structure. In this comparison of the two instruments, we see that both of them were able to retrieve the PBL height, with a difference of about 50–100 m. This may be related to the weaker signals retrieved by the ceilometer, compared to those of the lidar (Markowicz et al., 2008). Moreover, the radiosonde data obtained that day (27 November at 12:00 UTC) showed that the PBL height was indeed around 1300–1400 m a.s.l. (first knee with intense negative gradient of the relative humidity and the positive gradient of the potential temperature), which is in very good accordance with the lidar measurements.

4 Inter-comparison of aerosol backscatter coefficients obtained by lidar and ceilometer measurements

In this study we also inter-compared the aerosol backscatter profiles obtained by the three laser remote sensors (two lidars and one ceilometer). The lidar system provided by Raymetrics S.A. was used as a reference system for comparing the vertical profiles

AMTD
4, 73–99, 2011

of the aerosol backscatter coefficient. The main drawback of this inter-comparison was that the Raymetrics lidar and the CL31 ceilometer were running at two different wavelengths. The ceilometer operates in the infrared (910 nm) while the lidar operates in the ultraviolet (355 nm). In order to overcome this obstacle and reduce the spectral conversion errors, we used sun photometer data from the multi-filter radiometer (UV-MFR) to estimate the so-called backscatter-related Ångström exponent. The conversion of the ceilometer's backscatter coefficient to the ultraviolet spectral area was applied according to the formula:

$$c_{(z)} = -\frac{\ln\left(\frac{b_{\lambda_1}}{b_{\lambda_2}}\right)}{\ln\left(\frac{\lambda_1}{\lambda_2}\right)} \quad (1)$$

Equation (1) leads to the following conversion:

$$b_{\lambda_1} = e^{-\ln\left(\frac{\lambda_1}{\lambda_2}\right)\cdot c(z)} b_{\lambda_2} \quad (2)$$

where λ_1=355 or 1064 nm and λ_2=910 nm are the emitted wavelengths, while b_{λ_1} and b_{λ_2} are the corresponding backscatter coefficients at altitude z. In lidar terminology $c(z)$ is the so-called color index and equals to the Ångström exponent related to backscatter, which indicates the size of the scattering aerosols. The calculated values of the Ångström exponent (Michalsky et al., 2001) for the days into consideration using measurements of the aerosol optical depth (AOD) obtained by the UV-MFR radiometer were found to be 1.979 for 26 November and 0.369 for 27 November.

In Fig. 4a and b we present the results of the comparison of the aerosol backscatter coefficient profiles obtained by the Raymetrics (at 355 nm) and Vaisala (converted to 355 nm data) instruments for 26 and 27 November. Since the ceilometer's output energy is low we had to perform a 3-h average in order to sufficiently reduce the noise in the backscatter coefficient profiles obtained by the instrument. This method was followed in all the ceilometer backscatter coefficient profiles presented in this study. For the lidar measurements we averaged only one hour profiles as shown in Fig. 4a and b.

AMTD
4, 73–99, 2011

From Fig. 4a and b we see that the inter-comparison of the retrieved aerosol backscatter vertical profiles is quite satisfactory from 500 m (above the full overlap height) up to 5000 m height asl., except for 26 November, where the Raymetrics lidar shows much higher aerosol backscatter values below 1100 m than the ceilometer (the mean difference is of the order of 33%). This may be attributed to the unsatisfactory retrieval of the $c(z)$ value (due to mixture of different aerosol types) to perform the conversion of the aerosol backscatter coefficient from the near infrared to the ultraviolet spectral region. In the following section we present an inter-comparison analysis between the NTUA and the ceilometer retrieved vertical aerosol backscattered profiles obtained during two different aerosol conditions over Athens (biomass burning and Saharan dust event).

4.1 Case studies

4.1.1 Forest fire (biomass burning) smoke aerosols

On 23 July 2009 during scheduled measurements within EARLINET, an intense aerosol layer was detected by the NTUA Raman lidar system. This layer (about 500–1000 m thickness) appeared over Athens at the altitude of 3500 m (around 02:40 UTC) and started to descend during the night, merging with the convective PBL located around 2200 m at about 12:00 UTC. In Fig. 5 we present the temporal evolution of the range-corrected lidar signal obtained at 1064 nm. According to the Hysplit model (Draxler and Rolph, 2003), the origin of the air masses arriving over Athens at various levels (2000 m, 3000 m and 4000 m) at 12:00 UTC on that day overpassed the Balkan area, only one day earlier (Fig. 6). It seems that these air masses were enriched by biomass burning particles emitted from forest fires in Romania, as corroborated by the corresponding ESA/ATSR data (the orange points indicating the active hot spots from biomass burning sites).

Figure 7 shows the averaged vertical profiles of the aerosol backscatter coefficient obtained by the NTUA Raman lidar (at 1064 nm) and the ceilometer (converted to

AMTD
4, 73–99, 2011

1064 nm data). As shown in Fig. 7 both instruments recorded on 24 July a very intense aerosol layer over Athens extending from 2000 m up to 3300 m. The backscatter-related Ångström exponent value used for the wavelength conversion of the ceilometer backscatter coefficient profile from 910 nm to 1064 nm was found to be 1.59 and was calculated as described previously. The maximum value of the backscatter coefficient within this layer was $2\times10^{-6}\,m^{-1}\,sr^{-1}$ according to the ceilometer and $1.35\times10^{-6}\,m^{-1}\,sr^{-1}$ according to the NTUA lidar system. This difference can be attributed to the fact that these two systems were not collocated, since the ceilometer was located on the Pnyx hill, while the lidar was located inside the NTUA Campus at a distance of 6 km. In any case the mean difference between the two vertical profiles was of the order of 32%.

4.1.2 Desert dust aerosols

On 1 June 2009, the NTUA Raman lidar system detected several aerosol layers over Athens. Two strong and stable layers were detected around 3750 m and 2000 m, while less intense layers were found around 4500 m and 5000 m. On that day simultaneous measurements were performed by the NTUA Raman lidar system and NOA ceilometer. In Fig. 8 we present the temporal evolution of the range-corrected lidar signal (in A.U.) at 1064 nm as obtained by the NTUA Raman lidar system on 1 June 2009 (12:02–13:19 UTC). In Fig. 8 we can see that the aerosol layer around 2000 m merges with the convective PBL around 13:00 UTC. To identify the origin of the air masses sampled over Athens at various heights, that were very rich in particles, we run the Hysplit model again (Fig. 9). Indeed the 4-day air mass back-trajectories showed that the origin of the particles detected over Athens was from the Central and Western Saharan deserts, which explains the intense aerosol layers detected.

In Fig. 10 we examine the corresponding aerosol backscatter coefficient profiles obtained by the two instruments (the lidar data were averaged over one hour, while the ceilometer data over two hours; all averages were made around 12:00 UTC). The ceilometer vertical profile of the aerosol backscatter coefficient obtained originally at

AMTD
4, 73–99, 2011

910 nm was converted to the wavelength of the NTUA lidar (1064 nm) according to Eq. (2). The backscatter-related Ånström exponent used for the calculation was 0.880 and was found using the AOD data obtained by the UV-UV-MFR radiometer (at 368 nm and 940 nm). As it can be observed in Fig. 10 the aerosol layers were recorded by both instruments and were in generally in good agreement. At the peak of the layer A the values of the backscatter coefficient measured by the two instruments were almost identical approximately equal to 3.2×10^{-6} ($m^{-1}\,sr^{-1}$). At the peaks of the more intense layers B and C the ceilometer data showed higher values than the ones obtained by the lidar system. For layer B the peak values obtained by the ceilometer and the lidar were 5.9×10^{-6} ($m^{-1}\,sr^{-1}$) and 4.16×10^{-6} ($m^{-1}\,sr^{-1}$), respectively at 4.7 km. Layer C was lying at 5.7 km and the corresponding values of the ceilometer and the lidar were 5.9×10^{-6} ($m^{-1}\,sr^{-1}$) and 3.5×10^{-6} ($m^{-1}\,sr^{-1}$), respectively. As can be seen in Fig. 10 the ceilometer shows approximately much higher values of the backscatter coefficient at layers B and C.

This can be attributed (as discussed previously) to the fact that layers B and C are intense and thus an unsatisfactory retrieval of the Ångström exponent related to backscatter, in high aerosol loads, may result in higher uncertainties on the retrieved backscatter coefficient profile. Moreover, since our measurements were taken during daytime we did not have Raman lidar measurements in order to obtain the exact lidar ratio profile (Ansmann et al., 1992). Thus, for our lidar calculations we used a lidar ratio of 60 sr typical for Sahara dust episodes over Athens (Papayannis et al., 2005, 2008) which introduces an extra error parameter in the retrieved aerosol backscatter coefficient profile values calculated by the lidar method. An additional uncertainty is introduced by the use of a lidar ratio of 30 sr used by default by the ceilometer, which may explain the difference found between the two aerosol backscatter profiles. Finally, the distance of 6 km between the two sounding sites, may not play a crucial role in this kind of large-scale Saharan dust transport events. In any case the mean difference between the two vertical profiles, below 4000 m height (layer A), was of the order of 17%, while for the layers B and C was found to be 84%.

AMTD
4, 73–99, 2011

5 Summary and conclusions

In this paper we showed the inter-comparison of two active remote sensors (lidar and ceilometer) in determining the structure of the PBL and in retrieving the tropospheric aerosol vertical profiles over Athens, Greece. This was performed under strongly different atmospheric conditions (urban air pollution, biomass burning and Saharan dust event). We showed that in general a good agreement was found in determining these two parameters, especially when collocated measurements were performed (a difference of about 50–100 m in retrieving the PBL height and about 5–33% in the case of the aerosol backscatter coefficients inter-comparison). This difference may be attributed mainly to an unsatisfactory retrieval of the backscatter-related Ångström exponent, and less to the much weaker signal of the ceilometer compared to the lidar system. It was also found that the Vaisala CL31 ceilometer was able to detect correctly the presence of various aerosol layers under strongly different aerosol concentrations (urban air pollution, biomass burning and Saharan dust event). Moreover, we found that the conversion of the ceilometer data from the near infrared to the ultraviolet region, to be comparable to the lidar data, gave quite satisfactory results.

Acknowledgements. The Hellenic National Meteorological Service (HNMS) is gratefully acknowledged for the provision of the radiosonde data. The authors gratefully acknowledge the NOAA Air Resources Laboratory (ARL) for the provision of the HYSPLIT transport and dispersion model and/or READY website (http://www.arl.noaa.gov/ready.php) used in this publication. Hot spot fire data were provided by the ATSR/ESA satellite.

References

Amiridis, V., Balis, D. S., Kazadzis, S., Giannakaki, E., Papayannis, A., and Zerefos, C.: Four-year aerosol observations with a Raman lidar at Thessaloniki, Greece, in the framework of EARLINET, J. Geophys. Res., 110, D21203, doi:10.1029/2005JD06190, 2005.

Amiridis, V., Melas, D., Balis, D. S., Papayannis, A., Founda, D., Katragkou, E., Giannakaki, E., Mamouri, R. E., Gerasopoulos, E., and Zerefos, C.: Aerosol Lidar observations and model

AMTD
4, 73–99, 2011

calculations of the Planetary Boundary Layer evolution over Greece, during the March 2006 Total Solar Eclipse, Atmos. Chem. Phys., 7, 6181–6189, doi:10.5194/acp-7-6181-2007, 2007.

Amiridis, V., Balis, D. S., Giannakaki, E., Stohl, A., Kazadzis, S., Koukouli, M. E., and Zanis, P.: Optical characteristics of biomass burning aerosols over Southeastern Europe determined from UV-Raman lidar measurements, Atmos. Chem. Phys., 9, 2431–2440, doi:10.5194/acp-9-2431-2009, 2009.

Angelou, N., Papayannis, A., Mamouri, R. E., Amiridis, V., and Tsaknakis, G.: On the relation between aerosol backscatter and atmospheric relative humidity in an urban area over Athens, Greece by using Raman lidar and radiosonde data, Int. J. Remote Sens., in press, 2011.

Ansmann, A., Wandinger, U., Riebesell, M., Weitkamp, C., Michaelis, W.: Independent measurement of extinction and backscatter profiles in cirrus clouds by using a combined Raman elastic-backscatter lidar, Appl. Optics, 31, 7113–7131, 1992.

Böckmann, C., Wandinger, U., Ansmann, A., Bösenberg, J., Amiridis, V., Boselli, A., Delaval, A., De Tomasi, F., Frioud, M., Grigorov, I. V., Hågård, A., Horvat, M., Iarlori, M., Komguem, L., Kreipl, S., Larchevêque, G., Matthias, V., Papayannis, A., Pappalardo, G., Rocadenbosch, F., Rodrigues, J. A., Schneider, J., Shcherbakov, V., and Wiegner, M.: Aerosol lidar inter-comparison in the framework of the EARLINET project: Part II – Aerosol backscatter algorithms, Appl. Optics, 43, 977–989, 2004.

Draxler, R. R. and Rolph, G. D.: HYSPLIT (HYbrid Single-Particle Lagrangian Integrated Trajectory) Model Access via NOAA ARL READY Website, NOAA Air Resources Laboratory, Silver Spring, MD, 2003.

Endlich, R. M., Ludwig, F., and Uthe, E. E.: An automated method for determining the mixing layer depth from lidar observations, Atmos. Environ., 13, 1051–1056, 1979.

Eresmaa, N., Karppinen, A., Joffre, S. M., Räsänen, J., and Talvitie, H.: Mixing height determination by ceilometer, Atmos. Chem. Phys., 6, 1485–1493, doi:10.5194/acp-6-1485-2006, 2006.

Heese, B., Flentje, H., Althausen, D., Ansmann, A., and Frey, S.: Ceilometer lidar comparison: backscatter coefficient retrieval and signal-to-noise ratio determination, Atmos. Meas. Tech., 3, 1763–1770, doi:10.5194/amt-3-1763-2010, 2010.

Klett, J. D.: Stable analytical inversion solution for processing lidar returns, Appl. Optics, 20, 211–220, 1981.

AMTD
4, 73–99, 2011

Mamouri, R. E., Papayannis, A., Tsaknakis, G., and Amiridis, V.: 6-month ground-based water vapour Raman lidar measurements over Athens, Greece and system validation, J. Optoelectron. Adv. M., 9, 3546–3548, 2007.
Markowicz, K. M., Flatau, P. J., Kardas, A. E., Remiszewskaj, J., Stelmaszcyk, K., and Wöste, L.: Ceilometer retrieval of the boundary layer vertical aerosol extinction structure, J. Atmos. Ocean. Tech., 25, 928–944, 2008.
Martucci, G., Milroy, C., and O'Dowd, C. D.: Detection of cloud-base height using Jenoptik CHM15K and Vaisala CL31 ceilometers, J. Atmos. Ocean. Tech., 27, 305–318, 2010.
Matthias, V., Bösenberg, J., Freudenthaler, V., Balin, I., Balis, D., Bsenberg, J., Chaikovsky, A., Chourdakis, G., Comeron, A., Delaval, A., De Tomasi, F., Eixmann, R., Hågård, A., Komguem, L., Kreipl, S., Matthey, R., Rizi, V., Rodrigues, J. A., Wandinger, U., and Wang, X.:: Aerosol lidar inter-comparison in the framework of the EARLINET project, 1. Instruments, Appl. Optics, 43, 961–976, 2004.
McKendry, I. G., van der Kampa, D., Strawbridge, K. B., Christen, A., and Crawford, B.: Simultaneous observations of boundary-layer aerosol layers with CL31 ceilometer and 1064/532 nm lidar, Atmos. Environ., 43, 5847–5852, 2009.
Menut, L., Flamant, C., Pelon, J., and Flamant, P. H.: Urban boundary-layer height determination from lidar measurements over the Paris area, Appl. Optics, 38, 945–954, 1999.
Michalsky, J., Schlemmer, J., Berkheiser, W., Berndt, J., Harrison, L., Laulainen, N., Larson, N., and Barnard, J.: Multiyear measurements of aerosol optical depth in the atmospheric radiation measurement and quantitative links programs, J. Geophys. Res., 106, 12099–12107, 2001.
Papayannis, A. and Balis, D.: Study of the structure of the lower troposphere over Athens using a backscattering lidar during the MEDCAPHOT-TRACE Experiment: Measurements over a suburban area, Atmos. Environ., 32, 2161–2172, 1998.
Papayannis, A., Balis, D., Amiridis, V., Chourdakis, G., Tsaknakis, G., Zerefos, C., Castanho, A. D. A., Nickovic, S., Kazadzis, S., and Grabowski, J.: Measurements of Saharan dust aerosols over the Eastern Mediterranean using elastic backscatter-Raman lidar, spectrophotometric and satellite observations in the frame of the EARLINET project, Atmos. Chem. Phys., 5, 2065–2079, doi:10.5194/acp-5-2065-2005, 2005.
Papayannis, A., Amiridis, V., Mona, L., Tsaknakis, G., Balis, D., Bösenberg, J., Chaikovski, A., De Tomasi, F., Grigorov, I., Mattis, I., Mitev, V., Müller, D., Nickovic, S., Pérez, C., Pietruczuk, A., Pisani, G., Ravetta, F., Rizi, V., Sicard, M., Trickl, T., Wiegner, M., Gerd-

AMTD
4, 73–99, 2011

ing, M., Mamouri, R. E., D'Amico, G., and Pappalardo, G.: Systematic lidar observations of Saharan dust over Europe in the frame of EARLINET (2000–2002), J. Geophys. Res., 113, D10204, doi:10.1029/2007JD009028, 2008.

Papayannis, A., Mamouri, R. E., Amiridis, V., Kazadzis, S., Pèrez, C., Tsaknakis, G., Kokkalis, P., and Baldasano, J. M.: Systematic lidar observations of Saharan dust layers over Athens, Greece in the frame of EARLINET project (2004–2006), Ann. Geophys., 27, 3611–3620, doi:10.5194/angeo-27-3611-2009, 2009.

Pappalardo, P., Amodeo, A., Pandolfi, M., Wandinger, U., Ansmann, A., Bösenberg, J., Matthias, V., Amiridis, V., De Tomasi, F., Frioud, M., Iarlori, M., Komguem, L., Papayannis, A., Rocadenbosch, F., and Wang, X.:: Aerosol lidar inter-comparison in the framework of the EARLINET project, 3. Raman lidar algorithm for aerosol extinction, backscatter and lidar ratio, Appl. Optics, 43, 5370–5385, 2004.

Seinfeld, J. H. and Pandis, S. N.: Atmospheric Chemistry and Physics, from Air Pollution to Climate Change, 2nd edn., John Wiley, New York, 2006.

Stull, R. B.: An Introduction to Boundary Layer Meteorology, Kluwer Acad. Publishing, Dordrecht, The Netherlands, 1988.

Wang, X., Boselli, A., D'Avino, L., Pisani, G., Spinelli, N., Amodeo, A., Chaikovsky, A., Wiegner, M., Nickovic, S., Papayannis, A., Perrone, M. R., Rizii, V., Sauvage, L., and Stohl, A.: Volcanic dust characterization by EARLINET during Etna's eruptions in 2001–2002, Atmos. Environ., 42, 893–905, 2008.

AMTD
4, 73–99, 2011

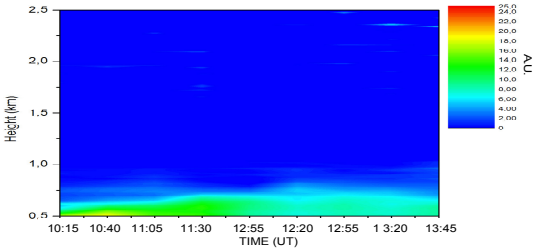

(a)

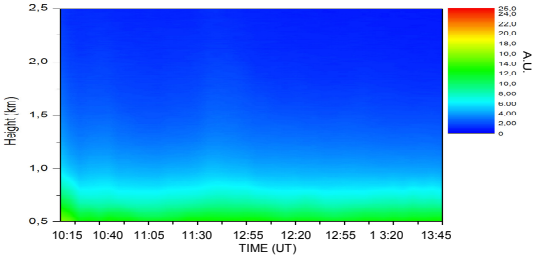

(b)

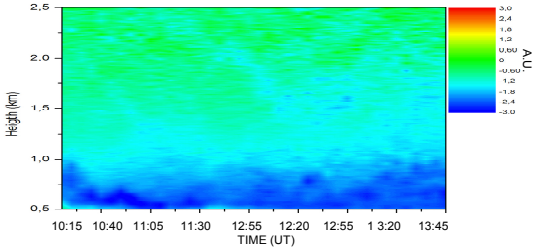

(c)

Fig. 1. Backscattered signal obtained by the ceilometer **(a)**, range-corrected **(b)** and first derivative of the logarithm **(c)** of the backscattered lidar signal obtained by the Raymetrics S.A. lidar system from 10:15 to 13:45 UTC on 26 November 2008 (in A.U.).

AMTD
4, 73–99, 2011

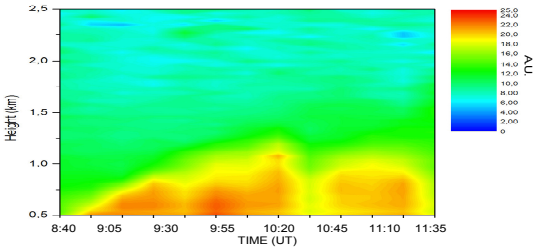

(a)

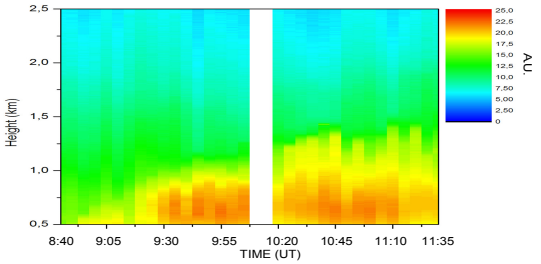

(b)

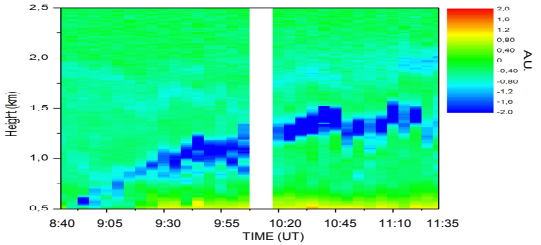

(c)

Fig. 2. Backscattered signal obtained by the ceilometer **(a)**, range-corrected **(b)** and first derivative of the logarithm **(c)** of the backscattered lidar signal obtained by the Raymetrics S.A. lidar system from 08:40 to 11:35 UTC on 27 November 2008 (in A.U.).

AMTD
4, 73–99, 2011

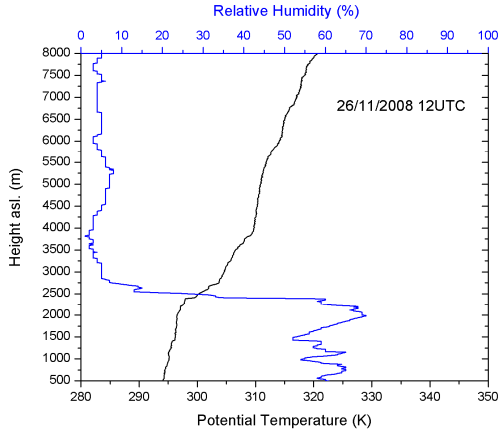

(a)

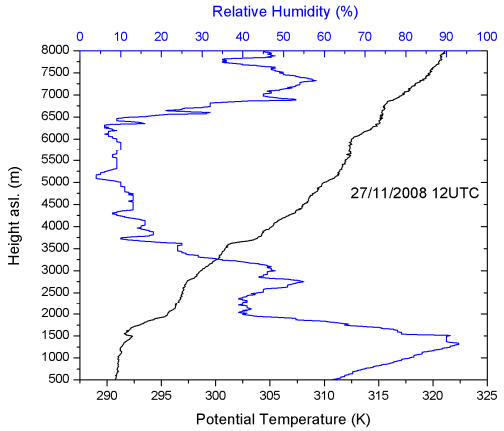

(b)

Fig. 3. Radiosonde data providing the vertical profile of the relative humidity (%) and potential temperature (K), at 12:00 UTC over Athens, on 26 November **(a)** and 27 November **(b)**, 2008.

AMTD
4, 73–99, 2011

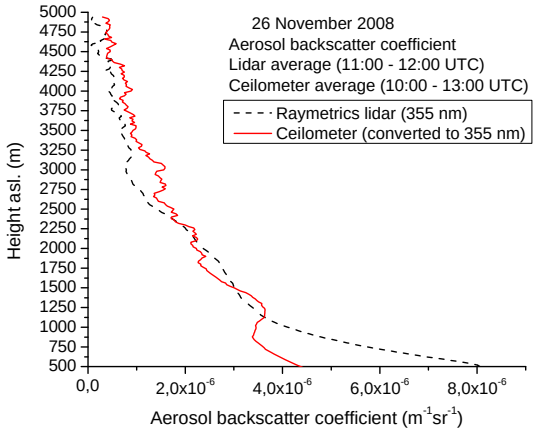

(a)

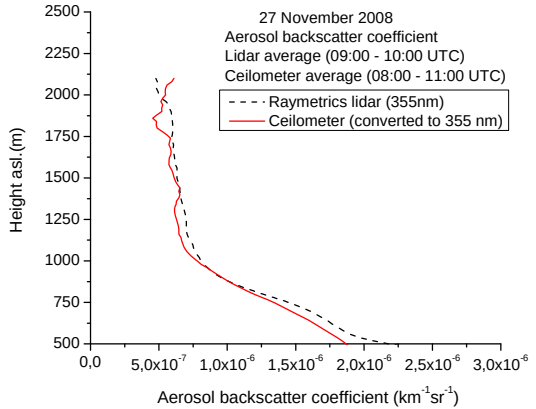

(b)

Fig. 4. Comparison of the aerosol backscatter coefficient profiles, obtained by the Raymetrics lidar and the ceilometer on 26 November **(a)** and 27 November 2008 **(b)**.

AMTD
4, 73–99, 2011

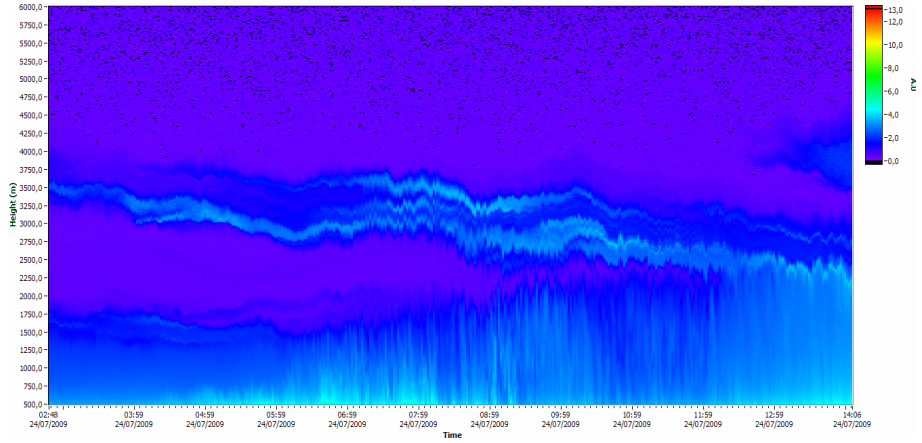

Fig. 5. Temporal evolution of the range-corrected lidar signal (in A.U.) at 1064 nm as obtained by the NTUA Raman lidar system on 24 July 2009 (02:48–14:06 UTC).

AMTD
4, 73–99, 2011

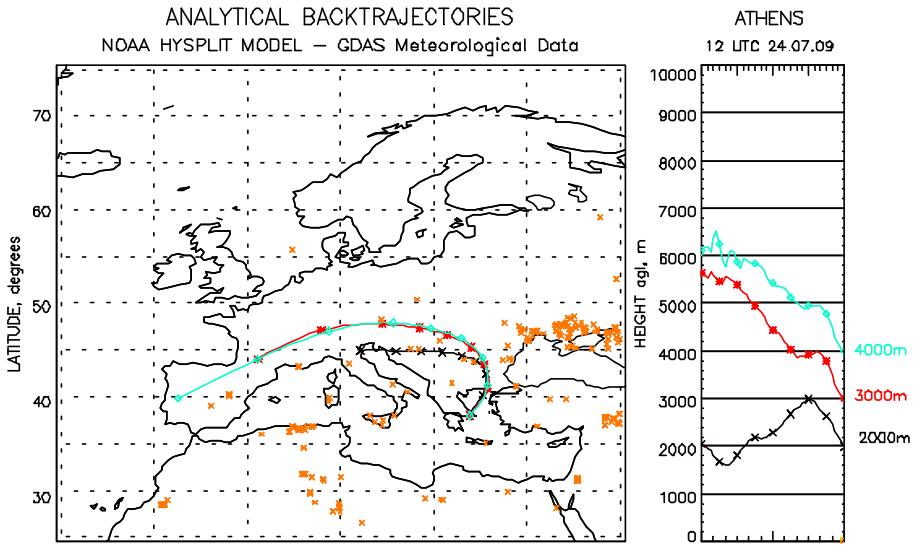

Fig. 6. Back-trajectories of air masses arriving over Athens on 24 July 2009 (12:00 UTC) at various heights (2000 m, 3000 m, 4000 m). The orange points indicate the active hot spots from biomass burning sites.

AMTD
4, 73–99, 2011

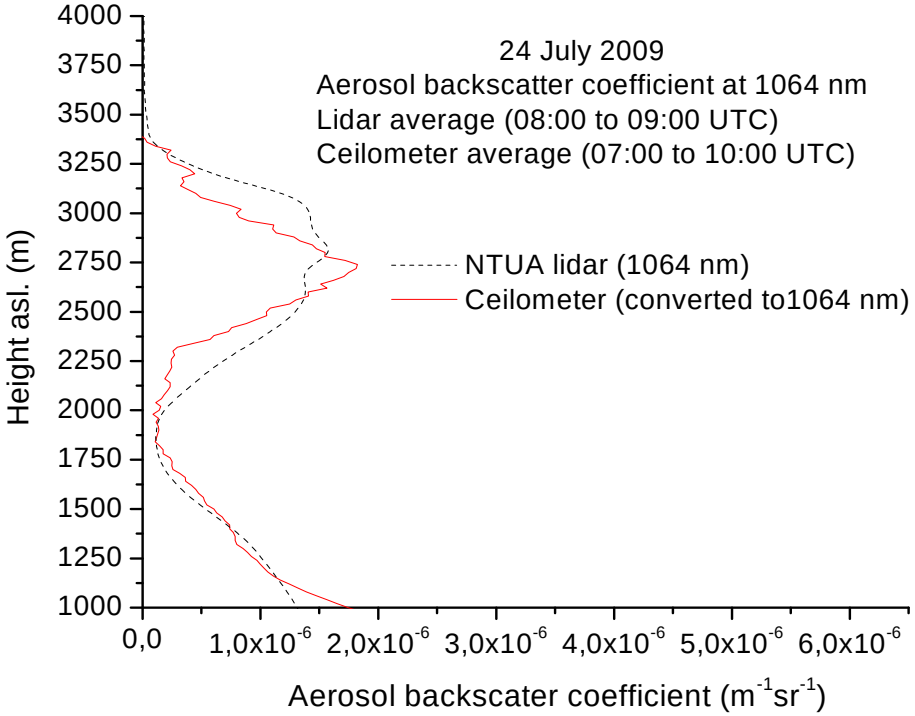

Fig. 7. Average vertical profiles of the aerosol backscatter coefficient obtained by the Vaisala ceilometer (07:00–10:00 UTC) and NTUA Raman lidar system (08:00–09:00 UTC) on 24 July 2009.

AMTD
4, 73–99, 2011

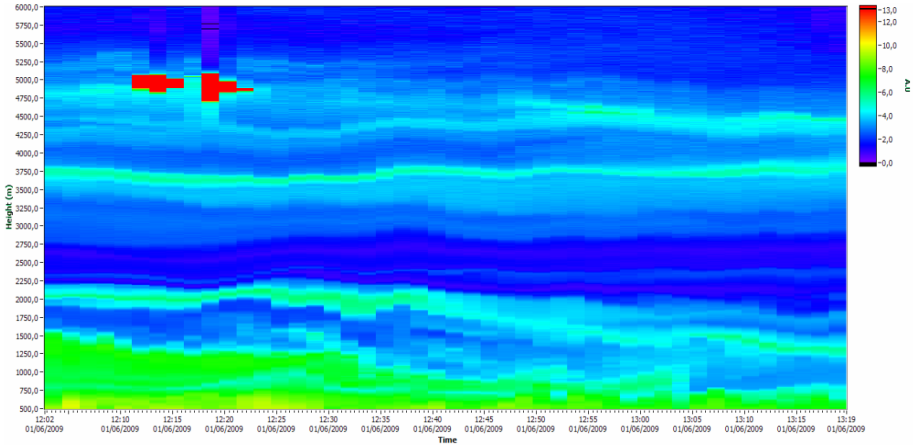

Fig. 8. Temporal evolution of the range-corrected lidar signal (in A.U.) at 1064 nm as obtained by the NTUA Raman lidar system on 1 June 2009 (12:02–13:19 UTC).

AMTD
4, 73–99, 2011

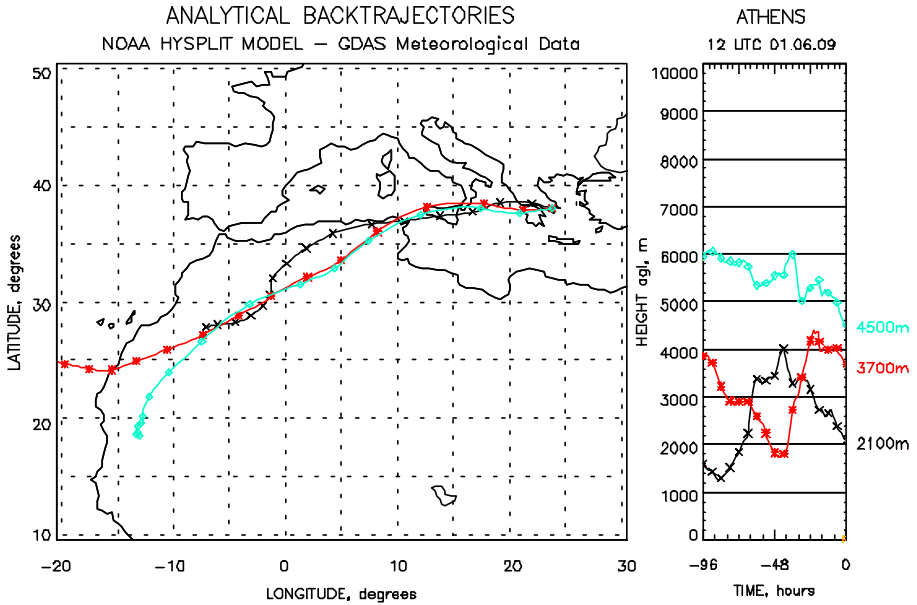

Fig. 9. Back-trajectories of air masses arriving over Athens on 1 June 2009 (12:00 UTC) at various heights (2100 m, 3700 m, 4500 m).

AMTD
4, 73–99, 2011

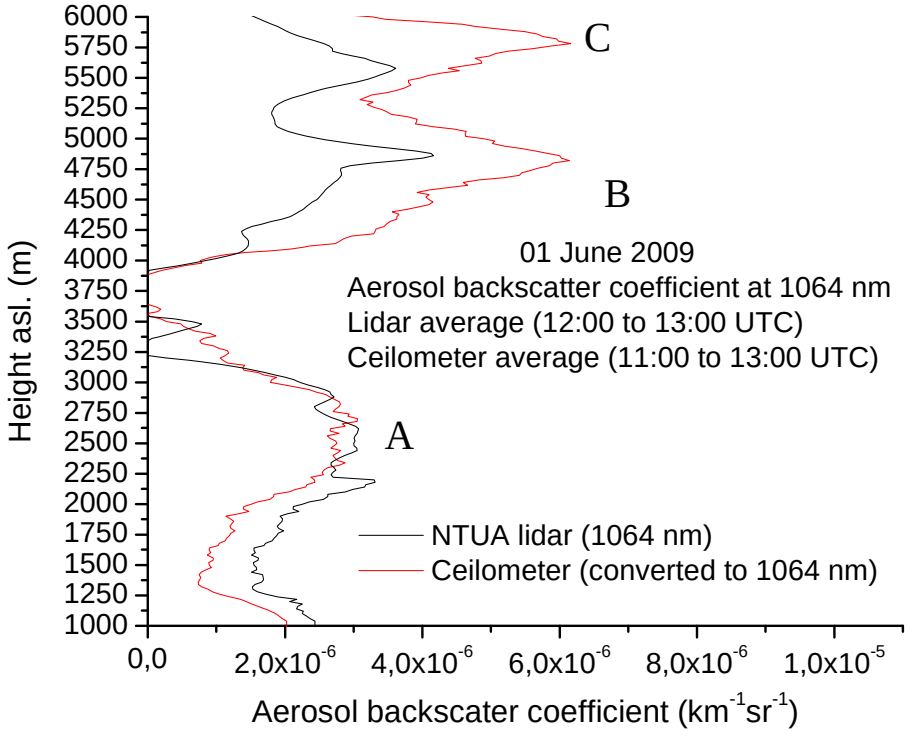

Fig. 10. Aerosol backscatter coefficient profiles obtained by the Vaisala ceilometer (11:00–13:00 UTC) and the NTUA Raman lidar system (12:00–13:00 UTC) on 1 June 2009.

AMTD
4, 73–99, 2011